AIP Conference Proceedings

Evidence of TiO_x reduction at the SiO_x/TiO_x interface of passivating electron-selective contacts

Cite as: AIP Conference Proceedings **1999**, 040005 (2018); https://doi.org/10.1063/1.5049268
Published Online: 10 August 2018

Jinyoun Cho, Maarten Debucquoy, Maria Recaman Payo, et al.

View Online

Export Citation

ARTICLES YOU MAY BE INTERESTED IN

Titanium dioxide/silicon hole-blocking selective contact to enable double-heterojunction crystalline silicon-based solar cell
Applied Physics Letters **106**, 123906 (2015); https://doi.org/10.1063/1.4916540

Carrier-selective contacts for Si solar cells
Applied Physics Letters **104**, 181105 (2014); https://doi.org/10.1063/1.4875904

Hole-blocking titanium-oxide/silicon heterojunction and its application to photovoltaics
Applied Physics Letters **102**, 203901 (2013); https://doi.org/10.1063/1.4803446

Lock-in Amplifiers up to 600 MHz

Zurich Instruments

Watch

© 2018 Author(s).

AIP Publishing

Evidence of TiO_x Reduction at the SiO_x/TiO_x Interface of Passivating Electron-Selective Contacts

Jinyoun Cho[1,2,a)], Maarten Debucquoy[2], Maria Recaman Payo[2], Elie Schapmans[2]
Ivan Gordon[2], Jozef Szlufcik[2], and Jef Poortmans[1,2,3,4]

[1] KU Leuven, Kasteelpark Arenberg 10, B-3001 Leuven, Belgium
[2] imec, Kapeldreef 75, B-3001 Leuven, Belgium
[3] Universiteit Hasselt, Martelarenlaan 42, B-3500 Hasselt, Belgium
[4] EnergyVille, Thor Park 8310, B-3600, Genk, Belgium

[a)]Corresponding author: Jinyoun.cho@imec.be

Abstract. A TiO_x layer is well known as an electron-selective contact material because of its asymmetric band offsets with respect to c-Si. When applying TiO_x layers as passivating electron-selective contacts, forming sub-stoichiometric TiO_x is important to obtain a low contact resistivity because oxygen vacancies increase the conductivity of TiO_x and provide n-type doping effects. In this work, oxygen vacancies at SiO_x/TiO_x interfaces are investigated by atomic depth profiling of XPS measurements. Three kinds of TiO_x layers are studied grown by either e-beam evaporation, atomic layer deposition or sputtering on c-Si. In all three TiO_x samples, a resulting stack of c-Si/SiO_x/TiO_x could be noticed XPS measurements that show SiO_x peaks near the c-Si/TiO_x interface. Moreover, clear TiO_2 peaks, which can be measured at the surface of all three TiO_x layer types, gradually change to Ti or $TiSi_2$ peaks near the SiO_x/TiO_x interface. This indicates that many oxygen vacancies seem to exist at the SiO_x/TiO_x interface. This TiO_x reduction may contribute to the formation of a dipole and increased downward band bending resulting in a lower contact resistivity in the electron-selective contacts. As a result, hetero-junction solar cells with i-a-Si:H/TiO_x/Ca/Al contacts exhibit a significant series resistance reduction of about 40 % compared to solar cells with i-a-Si:H/Ca/Al contacts.

INTRODUCTION

One way of further increasing the conversion efficiency of solar cells is to introduce carrier-selective contacts in the device architecture. Typically, carrier selective contacts in silicon solar cells can be formed in three ways: (1) via doping in c-Si, (2) via an external band bending source, or (3) via a band offset using metal oxide layers [1,2]. For the third approach, titanium oxide (TiO_x) is a very interesting material due to its large ΔE_V offset and small ΔE_C offset to silicon [3]. Since TiO_2 is too resistive, sub-stoichiometric TiO_x is used which includes oxygen vacancies, typically prepared by annealing with metals (*e.g.,* Al and Ti [4–6]), or by only Ca deposition on TiO_x without annealing [7]. Moreover, an interfacial SiO_x layer has been found at the Si/TiO_x interface on c-Si [8] or on a-Si:H [9]. As to solar cells, high efficiencies above 20 % have been reported using SiO_x/TiO_x as an electron selective contact [10,11]. However, so far not much information is known about the nature of the SiO_x/TiO_x interface.

For these reasons, we investigated the stoichiometric evolution of TiO_x layers deposited by e-beam evaporation, atomic layer deposition (ALD) and sputtering. Moreover, the benefits of using TiO_x in ATOM (i-**a**-Si:H/**T**iOx/L**o**w work function **m**etal) contacts will be discussed.

EXPERIMENT

One-side-mirror-polished n-type Cz wafers (1 Ω·cm, 730 μm thickness) were used to study the Si/TiO_x interfaces. After HF-last cleaning, TiO_x layers were deposited by e-beam evaporation, ALD and sputtering. For e-beam evaporated TiO_x, TiO_2 pellets with O_2 flow were used to obtain stoichiometric TiO_2 [12] and, for ALD-TiO_x,

SiliconPV 2018, The 8th International Conference on Crystalline Silicon Photovoltaics
AIP Conf. Proc. 1999, 040005-1–040005-8; https://doi.org/10.1063/1.5049268
Published by AIP Publishing. 978-0-7354-1715-1/$30.00

$Ti(OCH_3)_4$ and H_2O were used as precursors [13]. Since process condition of the sputtered TiO_x was not found in the literature, the detailed process conditions used here were sputtering of a Ti target with Ar gas flow of 105 sccm, O_2 gas flow of 45 sccm, pressure of 3 mTorr and power of 2000 W.

After TiO_x layer deposition of about 10 nm thickness, a part of the samples were annealed in forming gas (FGA: 10 % H_2 in N_2) at 450 ºC for 30 minutes. X-ray photoelectron spectroscopy (XPS) was used to characterize the TiO_x. By using the Ar plasma, the atomic concentration was measured as a function of the depth from the top surface. A separate sample for a sputtered-TiO_x layer of 3 nm thickness was prepared to measure TEM to see the presence of interfacial SiO_x.

As to devices, front-junction silicon hetero-junction solar cells were prepared on Cz wafers (3.2 Ω·cm, 165 µm thick, textured on the front, polished on the rear). After i/p-a-Si:H stack on the front and i-a-Si:H deposition on the rear, TiO_x layers were deposited on the rear. Then, front side ITO was deposited by sputtering. A silver grid was printed only on the front for the test group while Ag was printed on both sides for the reference contact (i/n-a-Si:H/ITO/Ag). All cells were annealed at 175 ˚C using a belt furnace. For test structure groups, Al or Ca/Al was thermally evaporated. Therefore, three different solar cell structures were prepared(see, Figure 1). Detailed fabrication steps for making these silicon heterojunction (SHJ) solar cells can be found in [14]. Illuminated IV characteristics of these solar cells were measured with a solar simulator under standard conditions (AM1.5g, 1000 W m^{-2}, 25 °C).

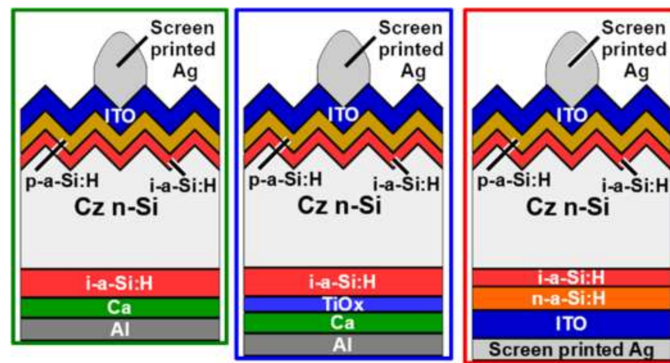

FIGURE 1. Schematic cross-sectional structures for the different solar cells with different electron-selective contacts [14].

RESULTS

Test Sample Results

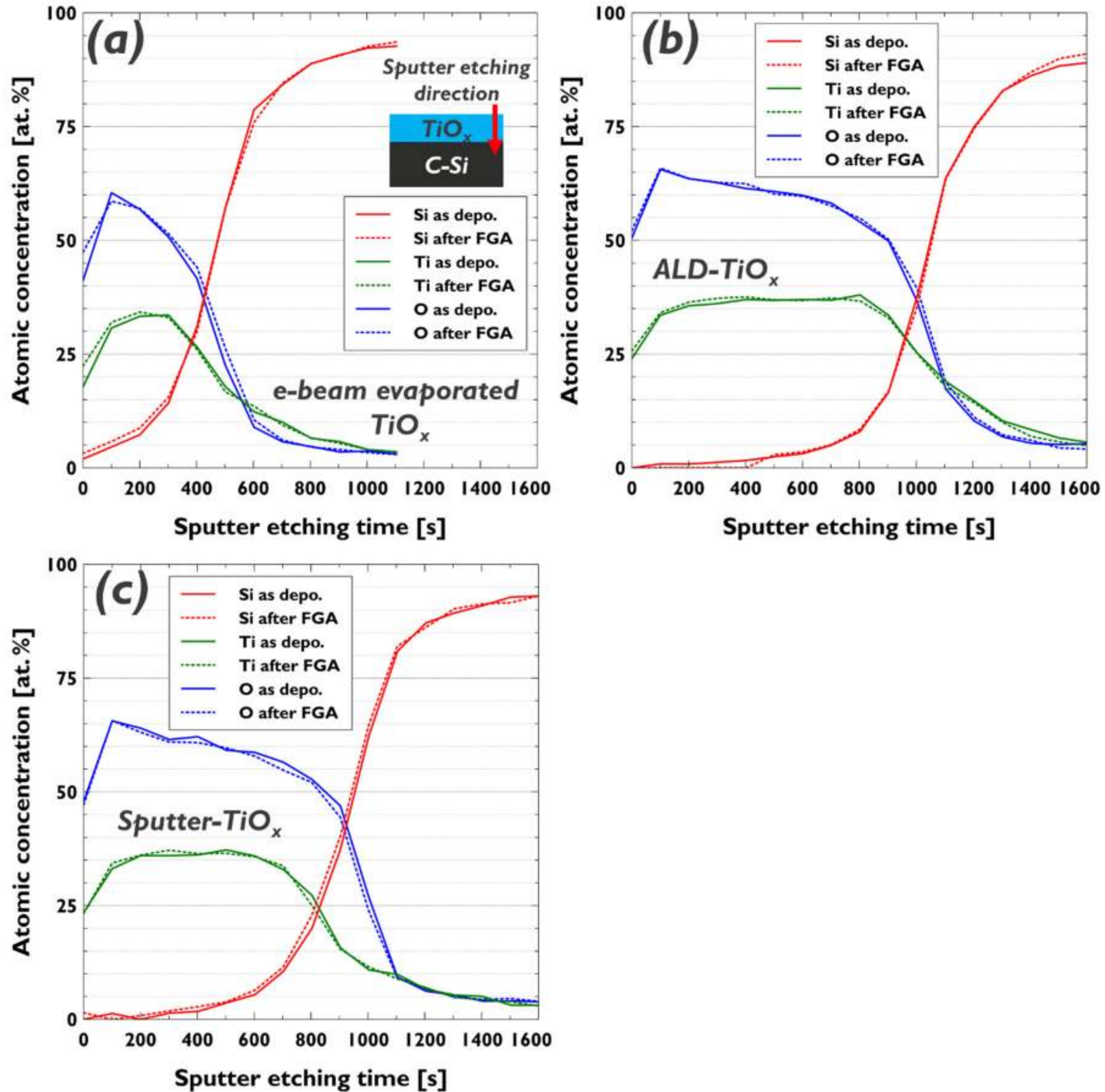

FIGURE 2. Atomic depth profile comparison of (a) e-beam evaporated-, (b) ALD- and (c) sputter-TiO_x before and after FGA.

Figure 2 shows the depth profiles of the different TiO_x layers before and after FGA. There is no significant difference in the XPS measurements before and after FGA. The total required Ar sputter etching time was shorter for the e-beam evaporated TiO_x compared to ALD- and sputter-TiO_x likely due to a thinner starting layer. Regarding the atomic profile of TiO_x before and after FGA, all three layers retain an atomic Ti:O ratio of about 1:2 near the top TiO_x surface. In case of the e-beam- and the ALD- TiO_x (see, Figure 2. (a) and (b)), there is a region where there is more Ti than O in Si while there is no such region in the sputtered TiO_x (see, Figure 2. (c)). Less diffusion of Ti into c-Si in the sputtered TiO_x might come from the thick diffusion barrier of SiO_x. Because the sputtered TiO_x has a larger gap at the right side of falling edge between of the Ti and of the O. A SiO_x thickness can be inferred based on this difference because of the high atomic concentration of Si and O in that region.

When zooming into the c-Si/TiO_x interface, the peaks in the XPS results (square marked area in Figures 3 (a) and (b)) indicate the presence of interfacial SiO_x at this interface for all three TiO_x deposition methods. For the sputter-TiO_x, with the highest Si-O peaks, the presence on an interfacial SiO_x layer of 1.4 nm (see, Figure 3 (c)), is confirmed by TEM. The TEM was not measured for the other layers, but it could be expected that a thinner SiO_x layer was formed underneath the TiO_x layer.Therefore, we actually fabricate SiO_x/TiO_x stacks during the TiO_x depositions.

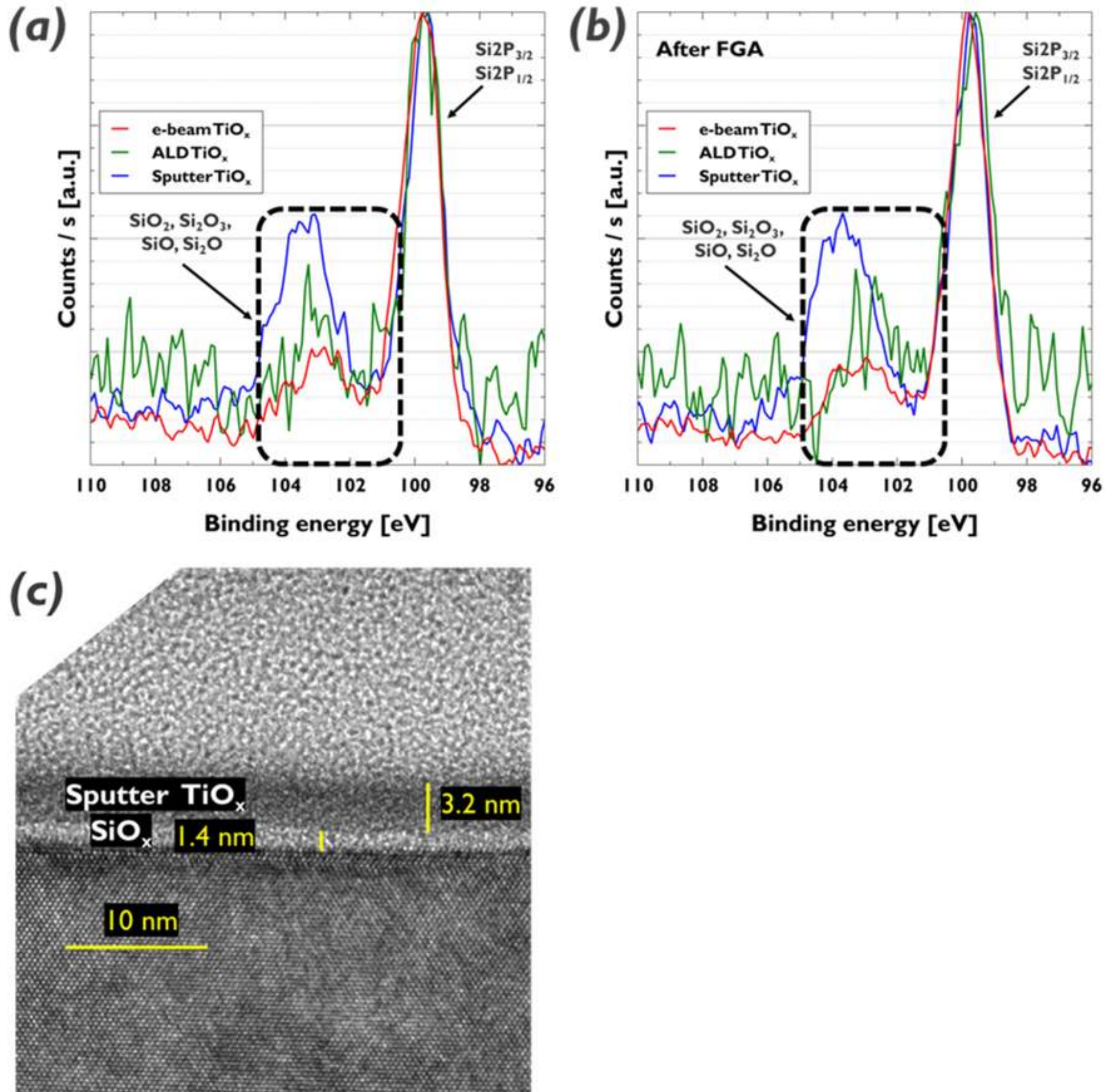

FIGURE 3. (a), (b) XPS results showing evidence of SiO_x formation at the Si/TiO_x interface before and after FGA (c) Cross-section TEM image of 3 nm thick TiO_x grown by sputtering (before FGA).

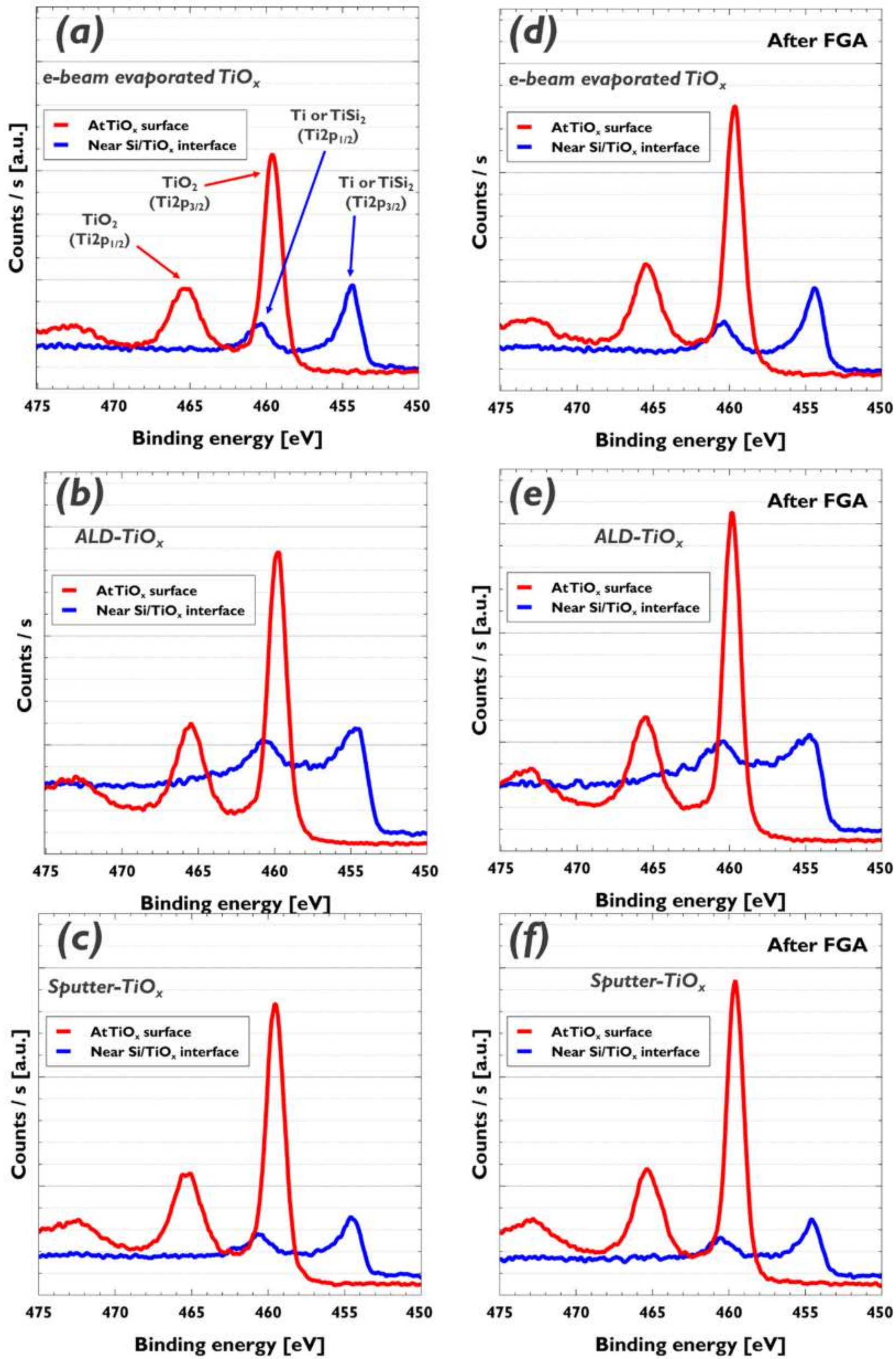

FIGURE 4. XPS peaks related to Ti measured at the TiO_x top surface (red) and near the Si/TiO_x interface (blue) before (a, b, c) and after FGA (d, e, f) using e-beam evaporated-(a, d), ALD (b,e) and sputter-TiO_x (c,f). Binding energy positions of TiO2, Ti or TiSi2 are marked in (a).

As can be seen in Fig. 4., the evolution of the Ti peak is very similar in all three TiO_x layers, and all peaks are at the same positions after forming gas anneals. At the surface, stoichiometric TiO_2 peaks are observed. However, as sputter etching time increases, the shape of the peaks gradually changes to that of TiO_x and eventually turns into the shape of Ti or $TiSi_2$ peaks (see, TABLE 1.).

TABLE 1. Binding energies of Ti, Ti-O, Ti-O_2 and $TiSi_2$.[15,16]

Bond	***Ti2p$_{1/2}$*** **[eV]**	***Ti2p$_{3/2}$*** **[eV]**
Ti	459.9	453.8
TiO	462.4	456.5
TiO_2	464.8	458.1
$TiSi_2$	459.3	453.2

Since the peak positions of Ti and $TiSi_2$ are very close each other, it is very difficult to determine the resulting chemical bond. This peak shift from TiO_2 to Ti or $TiSi_2$ implies that TiO_x near SiO_x could contain many oxygen vacancies which induce a doping effect by defect formation near the conduction band of TiO_x [17]. Moreover, it could be indirect evidence of dipole formation by the oxygen diffusion from TiO_x to SiO_x proposed by Kita et al. [18].

Cell Results

TABLE 2. Illuminated I-V parameters of champion cells with different electron-selective contacts. All SHJ cell data is from [14] except the result of the contact containing e-beam TiO_x.

Electron contact structure	J_{SC} [mA/cm2]	VOC [mV]	FF [%]	η [%]	R_S [Ω·cm^2]
i-a-Si:H / Ca / Al [14]	35.2	666.3	70.9	16.6	***3.2***
i-a-Si:H /e-beam-TiO_x / Ca / Al (ATOM)	34.8	674.1	71.8	16.9	***1.8***
i-a-Si:H /ALD-TiO_x / Ca / Al (ATOM) [14]	35.1	710.8	72.9	18.2	***2.0***
i-a-Si:H / n-a-Si:H / ITO / Ag (conventional SHJ) [14]	36.0	734.0	76.4	20.2	***1.7***

In the past, we achieved a reduction in contact resistivity of a-Si:H/Ca contacts by inserting a thin TiO_x layer between a-Si:H and Ca (the so-called ATOM (i-**a**-Si:H/**T**iO_x/L**o**w work function **m**etal) contact) [9]. This contact resistivity can be originated from several simultaneous influences; (1) The TiO_x reduces the pinning of the metal Fermi level thanks to a MIS (Metal-Insulator-Semiconductor) contact structure. In combination with (2) the low work function of the Ca, this reduces the Schottky barrier and so the contact resistivity. From the XPS study above, we learn that an SiO_x layer is formed in this ATOM contact between the TiO_x and the a-Si:H which might also assist in lowering the contact resistivity by (3) oxygen vacancy doping and (4) a dipole increasing the downward band bending.

While in [9] only contact resistivity structures where reported, here full cells with the ATOM structure are realized. Hence, the fill factor (FF) of the solar cells with ATOM contacts are higher than those of cells with i-a-Si:H/Ca/Al contacts thanks to a lower R_S (see, Table 2.), as determined by the Bowden method [19]. Since sputtering induces damage in the a-Si:H layer and results in a relatively thick interfacial SiO_x layer compared to the other two growth technique (see, Fig. 3), sputtered TiO_x was not integrated into the devices.

Although the conventional electron contact of silicon hetero-junction (SHJ) solar cells still outperforms our ATOM contact, our cell results are in the 2nd top ranked so far for cells with an electron-selective contact based on a-Si:H/TiO_x, most likely due to the low contact resistivity of the ATOM contact [20–23]. Currently, our solar cell efficiency is limited by the J_{SC} and the FF. Therefore, parasitic absorption in a-Si:H and ITO needs to be minimized, and further optimization of the electron selective contact is required to achieve a low R_S and an efficiency above 20%.

CONCLUSIONS

XPS and TEM measurements confirmed interfacial silicon oxide formation between silicon and TiO_x. Regardless of the TiO_x deposition technique, XPS measurements showed for all test samples Ti or TiSi peaks near the SiO_x/TiO_x interface while TiO_2 peaks were observed at the TiO_x surface. The Ti or the TiSi peaks near the SiO_x/TiO_x interface might be indirect evidence for oxygen movement which creates a dipole resulting in increased downward band bending at the contact. It is believed that in MIS contact structures with TiO_x, these dipoles and oxygen vacancies in TiO_x contribute to a R_S reduction of solar cells. This study may help to broaden the understanding about the nature of the Si/TiO_x interface.

ACKNOWLEDGMENTS

The authors gratefully acknowledge the financial support of imec's industrial affiliation program for Si-PV

REFERENCES

1. J. Melskens, B. W. H. van de Loo, B. Macco, M. F. J. Vos, J. Palmans, S. Smit, and W. M. M. Kessels, *in 2015 IEEE 42nd Photovolt. Spec. Conf.* "Concepts and prospects of passivating contacts for crystalline silicon solar cells," (IEEE, 2015) DOI 10.1109/PVSC.2015.7355646.
2. J. Melskens, B. W. H. van de Loo, B. Macco, L. E. Black, S. Smit, and W. M. M. Kessels, IEEE J. Photovoltaics **8**, 1–16 (2018) DOI 10.1109/JPHOTOV.2018.2797106.
3. J. Jhaveri, S. Avasthi, K. Nagamatsu, and J. C. Sturm, *in 2014 IEEE 40th Photovolt. Spec. Conf.* "Stable low recombination n-Si/TiO2 hole-blocking interface and its effect on silicon heterojunction photovoltaics," (IEEE, 2014) DOI 10.1109/PVSC.2014.6925206.
4. Y. Liu, Y. Chen, D. T. LaFehr, Y. Su, Y. Huo, Y. Kang, H. Deng, J. Jia, L. Zhao, M. Yuan, Z. Lyu, D. DeWitt, M. A. Vilgalys, K. Zang, X. Chen, C.-Y. Lu, T. I. Kamins, and J. S. Harris, *in SPIE Proc. Vol. 9749* "Titanium oxide electron-selective layers for contact passivation of thin-film crystalline silicon solar cells," F. H. Teherani, D. C. Look, and D. J. Rogers, Eds., (SPIE, 2016) DOI 10.1117/12.2213540.
5. H. Ali, X. Yang, K. O. Davis, K. Weber, and W. V Schoenfeld, Microsc. Microanal. **22**, 1600–1601 (2016) DOI 10.1017/S1431927616008849.
6. H. Yu, M. Schaekers, T. Schram, S. Demuynck, N. Horiguchi, K. Barla, N. Collaert, A. V.-Y. Thean, and K. De Meyer, IEEE Trans. Electron Devices **63**, 2671–2676 (2016) DOI 10.1109/TED.2016.2565565.
7. T. G. Allen, J. Bullock, Q. Jeangros, C. Samundsett, Y. Wan, J. Cui, A. Hessler-Wyser, S. De Wolf, A. Javey, and A. Cuevas, Adv. Energy Mater. **7**, 1602606 (2017) DOI 10.1002/aenm.201602606.
8. J. Melskens, R. W. H. S. Scheerder, W. J. H. Berghuis, B. W. H. Van De Loo, B. Macco, P. C. P. Bronsveld, P. Spinelli, and W. M. M. Kessels, *in EUPVSEC 2017* "Excellent silicon surface passivation by TiOx : aiming for electron selectivity by atomic layer deposition," (European PV solar energy Conference and Exhibition, Amsterdam, Netherland, 2017).
9. J. Cho, M. Debucquoy, M. Recaman Payo, S. Malik, M. Filipič, H. S. Radhakrishnan, T. Bearda, I. Gordon, J. Szlufcik, and J. Poortmans, *in SiliconPV Conf. 2017* ***124*** "Contact resistivity reduction on lowly-doped n-type Si using a low work function metal and a thin TiOx interfacial layer for doping-free Si solar cells," (2017) DOI 10.1016/j.egypro.2017.09.356.
10. X. Yang, K. Weber, Z. Hameiri, and S. De Wolf, Prog. Photovoltaics Res. Appl. **25**, 896–904 (2017) DOI 10.1002/pip.2901.
11. X. Yang, Q. Bi, H. Ali, K. Davis, W. V Schoenfeld, and K. Weber, Adv. Mater. **28**, 5891–5897 (2016) DOI 10.1002/adma.201600926.
12. W. Qiu, U. W. Paetzold, R. Gehlhaar, V. Smirnov, H.-G. Boyen, J. G. Tait, B. Conings, W. Zhang, C. B. Nielsen, I. McCulloch, L. Froyen, P. Heremans, and D. Cheyns, J. Mater. Chem. A **3**, 22824–22829 (2015) DOI 10.1039/C5TA07515G.
13. M. Popovici, J. Swerts, K. Tomida, D. Radisic, M.-S. Kim, B. Kaczer, O. Richard, H. Bender, A. Delabie, A. Moussa, C. Vrancken, K. Opsomer, A. Franquet, M. A. Pawlak, M. Schaekers, L. Altimime, S. Van Elshocht, and J. A. Kittl, Phys. status solidi - Rapid Res. Lett. **5**, 19–21 (2011) DOI 10.1002/pssr.201004462.
14. J. Cho, J. Melskens, M. Debucquoy, M. Recaman Payo, S. Jambaldinni, T. Bearda, I. Gordon, J. Szlufcik, W. M. M. Kessels, and J. Poortmans, Prog. Photovoltaics Res. Appl. 1–11 (2018) DOI 10.1002/pip.3023

15. K. Yokota and T. Yamada, Mater. Res. Innov. **2**, 103–109 (1998) DOI 10.1007/s100190050070.
16. W. Y. Yang, H. Iwakuro, H. Yagi, T. Kuroda, and S. Nakamura, Jpn. J. Appl. Phys. **23**, 1560–1567 (1984) DOI 10.1143/JJAP.23.1560.
17. X. Pan, M.-Q. Yang, X. Fu, N. Zhang, and Y.-J. Xu, Nanoscale **5**, 3601 (2013) DOI 10.1039/c3nr00476g.
18. K. Kita and A. Toriumi, Appl. Phys. Lett. **94**, 132902 (2009) DOI 10.1063/1.3110968.
19. S. Bowden and A. Rohatgi, *in 17th Eur. Photovolt. Sol. Energy Conf. Exhib.* "Rapid and accurate determination of series resistance and fill factor losses in industrial silicon solar cells," (Munich, Germany, 2001).
20. D. Sacchetto, Q. Jeangros, G. Christmann, L. Barraud, A. Descoeudres, J. Geissbuhler, M. Despeisse, A. Hessler-Wyser, S. Nicolay, and C. Ballif, *in 7th Int. Conf. Cryst. Silicon Photovoltaics 2017* "MoO_x and TiO_2 Carrier Selective Contacts for Dopant-free SHJs," (2017).
21. M. Boccard, X. Yang, K. Weber, and Z. C. Holman, *in 2016 IEEE 43rd Photovolt. Spec. Conf.* ***2016*** "Passivation and carrier selectivity of TiO2 contacts combined with different passivation layers and electrodes for silicon solar cells," (IEEE, 2016) DOI 10.1109/PVSC.2016.7750072.
22. H. Ali, X. Yang, K. Weber, W. V. Schoenfeld, and K. O. Davis, Microsc. Microanal. 1–5 (2017) DOI 10.1017/S1431927617012417.
23. J. Bullock, Y. Wan, Z. Xu, S. Essig, M. Hettick, H. Wang, W. Ji, M. Boccard, A. Cuevas, C. Ballif, and A. Javey, ACS Energy Lett. **3**, 508–513 (2018) DOI 10.1021/acsenergylett.7b01279.